Available online at www.sciencedirect.com
SCIENCE DIRECT®
Optics & Laser Technology 37 (2005) 532–540
Optics & Laser Technology
www.elsevier.com/locate/optlastec

Detecting and avoiding the necking deformation along polypropylene fibre axis using the fringe pattern analysis of multiple-beam microinterferometry

A.A. Hamza*, T.Z.N. Sokkar, K.A. EL-Farahaty, M.A.M. EL-Morsy, H.M. EL-Dessouky

Physics Department, Faculty of Science, Mansoura University, Mansoura 35516, Egypt

Received 16 January 2004; received in revised form 4 August 2004; accepted 18 August 2004
Available online 7 October 2004

Abstract

A fibre-drawing device attached with the system for producing multiple-beam Fizeau fringes in transmission is used to optimize the optical properties during the cold drawing of polypropylene (PP) fibres. This system is automated for interference pattern analysis. Two drawing processes for the PP fibres are applied and investigated. The first one is fast drawing in which the necking deformation is predicted and the other is the slow (step) drawing in which the necking can be avoided. The refractive index profiles ($n^{\parallel}$ and $n^{\perp}$) of PP fibres are determined at different positions along the fibre axis during the fast and slow drawing processes. The fibre interference patterns are automatically digitized and stored in a computer storage media. The slow drawing technique for PP fibres is recommended to overcome the deformation difficulties along the fibre axis due to necking during the drawing processes. Microinterferograms in case of light vibrating parallel and perpendicular to the fibre axis are given for illustration.

Keywords: Polypropylene fibres; Refractive index; Drawing; Necking deformation; Multiple-beam interferometry; Fringe pattern analysis

1. Introduction

Nowadays polymer-based fibres are becoming ubiquitous in a variety of high-tech applications, e.g. specialty coating, automotive, aerospace, semiconductors, composites, optics, etc. [1].

The cold drawing of a polycrystalline polymeric film induces a deep structural rearrangement as the initial morphology is transformed into the final fibrous organization. Since the transformation is irreversible and occurs under non-equilibrium thermodynamic conditions, the fibre obtained is a system in a metastable state. The consequence is the tendency of the newly formed system to relax from the metastable state to approach equilibrium. This drawing generates a new morphological unit, the microfibril, which is absent in the initial film. In the microfibril, crystalline blocks and amorphous layers are arranged with a regular alternating distribution along the sample axis [2].

Semi-crystalline polymers that crystallize under quiescent conditions often have a spherulitic morphology. The remarkable drawability of the semi-crystalline polymers makes it possible to high orient them in the solid state. Solid state processing techniques, such as drawing fibres or stretching films, depend upon the plastic deformation characteristics of the given polymer [3]. Upon uniaxial drawing, the spherulites are deformed to an ellipsoidal shape with the radial fibrils of the spherulites orienting in the drawing direction. However, the crystallites in the radial fibrils of the deformed spherulites generally tend to reorient with their chain axes along the drawing direction [4].

*Corresponding author. Tel.: +20-2-2708999; fax: +20-50-2246254.
E-mail address: hamzaaa@mans.edu.eg (A.A. Hamza).

0030-3992/$ - see front matter © 2004 Elsevier Ltd. All rights reserved.
doi:10.1016/j.optlastec.2004.08.010

Polypropylene (PP) fibres are composed of crystalline and non-crystalline regions. The spherulites developed from a nucleus can range in size from fractions of micrometre to centimetres in diameter. The *a*-axis of the crystal unit cell is aligned radially and the chain axis is homogeneously distributed in the planes perpendicular to this radial direction. Each crystal is surrounded by non-crystalline regions. Fibre spinning and drawing may cause the orientation of both crystalline and amorphous regions. If the extension is less than 0.5%, the spherulite deformation is elastic and no disruption of the structure occurs, otherwise spherulites are highly oriented in the direction of the force and finally are converted to micro-fibrils. These highly anisotropic micro-fibrillar structures lead to anisotropic fibre properties [5].

Studying the deformation mechanisms during uni-axial drawing of fibres is a useful task to characterize the opto-mechanical properties of textile fibres made from polymers materials [6]. In the particular case of semi-crystalline polymers, such as PP fibres, yielding and cold drawing contain two types of non-uniform deformation processes: the first one is the initiation of local necking and the other is the propagation of neck shoulders along the specimen. Both types result from the local instability of deformation but they are different in behaviour [cf. 7]. Using a new experimental technique based on a non-contact method for longitudinal deformation measurement, it was possible to detect the specific zone where neck initiation takes place, and to measure the inhomogeneous plastic deformation that is usually observed for semi-crystalline polymers undergoing tensile testing [7].

Walker [8] and Sova et al. [9] show that when some polymer sheets are drawn at low draw ratios, there is a narrowing of the thickness (called necking). They considered that the formation of these neck zones is due to microscopic inhomogeneities and to a large extent is a consequence of the orientation of polymer molecules. They also showed that there is a sudden structural transformation in the neck shoulder during solid-state drawing.

Necking or cold drawing is a smoothed jump in cross-sectional area of long and thin bars (filament or films) propagating with a constant speed. The necks in polymers, first observed about 70 years ago [10], are now commonly used in modern processing of polymer films and fibres. Qualitative structural models of necking have been intensively discussed in experimental papers. The most popular such a model proposed by Peterlin and Olf [11] considered the folded chain blocks in the necking of semi-crystalline polymers as tilted, sheared, broken off the lamellae and becoming incorporated in the (amorphous) microfibrils. Gent and co-workers [12–14] have recently proposed another model for semi-crystalline polymers. They related necking to the mechanism of unfolding chains in crystalline blocks and transferring them into amorphous phase with consequent orientation. This model explains the puzzling fact that the higher the degree of crystallinity, the higher the necking final drawing ratio. The drawing ratio is defined as the ratio between the new (stretched) length of the fibre to the initial length of this fibre.

In this paper, an opto-mechanical investigation for undrawn PP fibres will be performed using the fibre-drawing instrument [15] connected with the system for producing multiple-beam Fizeau fringes in transmission across the fibre. An automatic fringe analysis technique with software prepared specially for fibre characterization was used [16]. The refractive indices, in case of light vibrating parallel and perpendicular to the fibre axis ($n^{\parallel}$ and $n^{\perp}$) and their profiles of PP fibres will be determined along the fibre axis at different draw ratios. Two different types of the drawing processes (fast and slow drawing) are applied and investigated by determining the optical properties along the fibre axis during each type.

2. Necking phenomenon of polymeric fibres

The necking phenomenon usually occurs when a homogeneous solid polymeric bar (fibre or film) is stretched uniaxially [17,18]. In this case the polymer fibre is not deformed homogeneously. Instead, two almost uniform sections occur in the sample: one being nearly equal to its initial thickness and another being considerably thinner in the cross-sectional dimensions. These sections are jointed by a relatively short transition (necking) zone that propagates with a constant speed along the fibre as a stepwise wave in the direction of the fibre's thick end as shown in Fig. 1. The neck region of a fibre experiences a triaxial state of stress during the cold-drawing process. Draw ratio is directly related to the force applied during the drawing process. As the draw ratio is changed, the shape of the neck is altered. The force applied to the fibre during the drawing process is resolved into two components perpendicular and parallel to the neck. In Fig. 1, $F \sin\alpha$ is an

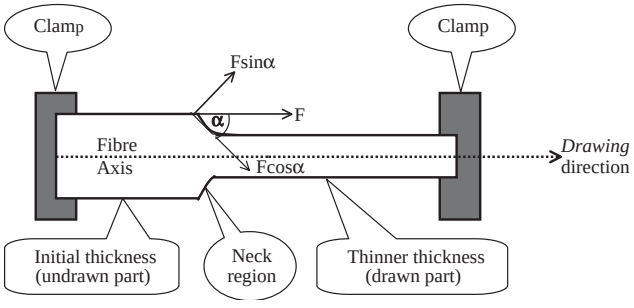

Fig. 1. Sketch of necking polymeric fibre sample [17].

outward-acting force and α is the neck angle. As the critical draw ratio (causes neck) is approached, the value of $F \sin\alpha$ is significantly increased relative to the value of $F \cos\alpha$. This increase in the outward force causes the material to fail at discontinuities in the structure, resulting in the formation of voids.

3. Experimental set-up and technique

The automated multiple-beam Fizeau fringe system is an accurate and non-destructive technique in the field of fibre research. The resulting fringes give qualitative and quantitative information about the optical and structural properties of the fibre under investigation. The technique has been used to determine the refractive index, birefringence and dispersion of man-made and optical fibres. Also this technique is capable of constructing the refractive index profile, which has strong effects on the group delay characteristics of fibres. The automated and high-speed image processing system is used to analyse the fringe pattern and give an accurate analysis. The principal method in the automatic fringe-pattern analysis is fringe skeleton extraction [19–21].

The automated opto-mechanical set-up used in this work consists of three basic units (see Fig. 2):

Interferometric unit [21]: This is the optical system for producing multiple-beam Fizeau fringes in transmission, which consists of (1) mercury lamp, (2) condenser, (3) iris diaphragm, (4) collimating lens, (5) polarizer, (6) monochromatic filter and (7) reflector.

Mechanical unit [15]: This is the fibre-drawing system, which consists of (8) threaded rod, $(9, 9')$ movable bar, $(10, 10')$ sliding rods, $(11, 11', 12, 12')$ fixed frame, $(13, 13')$ sliding bar, $(14, 14')$ fixed rods, (15) special clamp, (16) liquid wedge interferometer, (17) movable weight, (18) fixed microscope stage, (19) movable microscope stage, (20) micrometer screw, (21) pointer and (22) vernier.

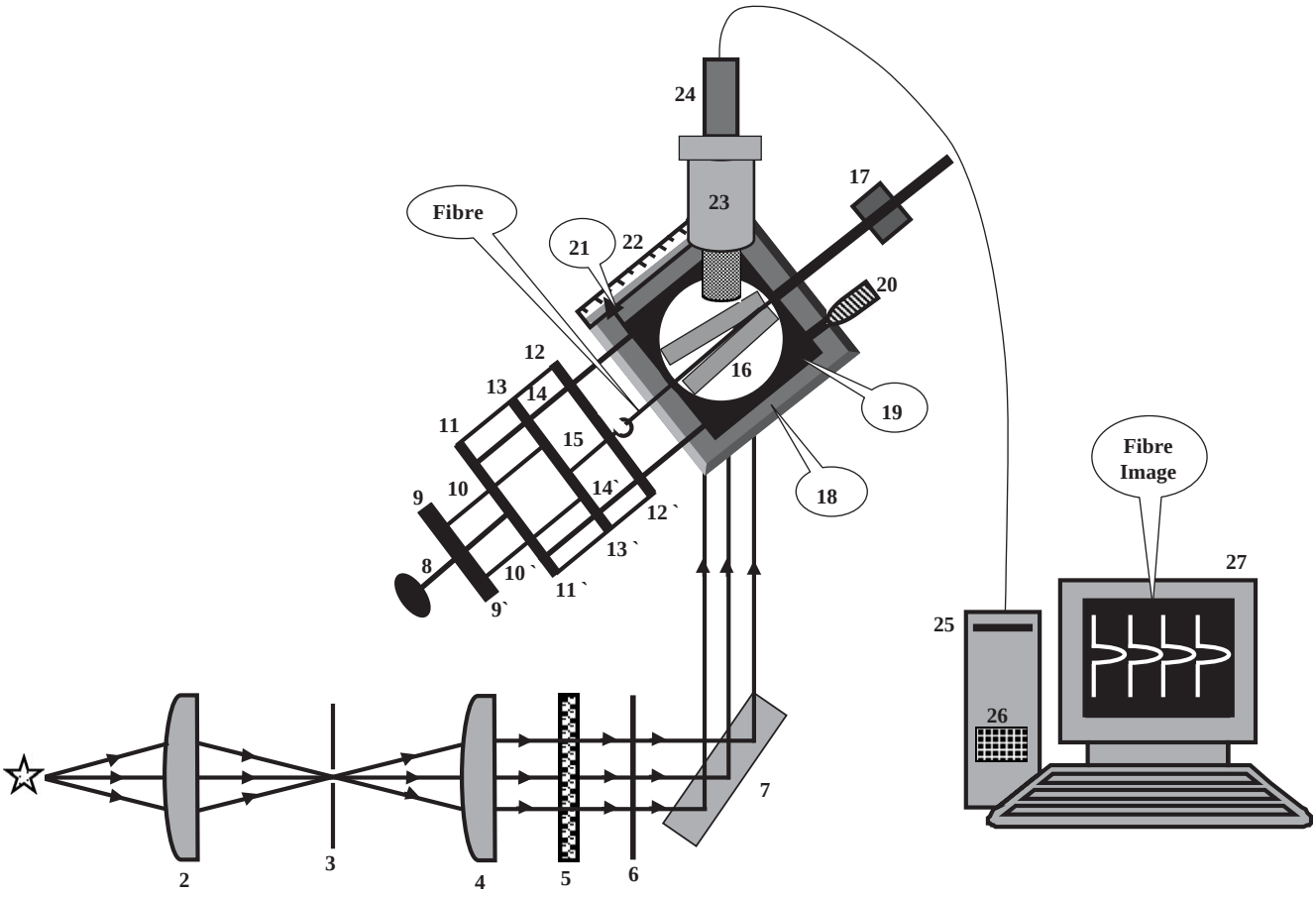

Fig. 2. Schematic diagram of the drawing device attached to the automated optical system for producing multiple-beam Fizeau fringes in transmission: 1 mercury lamp, 2 condenser lens, 3 iris diaphragm, 4 collimating lens, 5 polarizer, 6 monochromatic filter, 7 reflector, 8 threaded rod, $(9, 9')$ movable bar, $(10, 10')$ sliding rods, $(11, 11', 12, 12')$ fixed frame, $(13, 13')$ sliding bar, $(14, 14')$ fixed rods, 15 special clamp, 16 wedge interferometer, 17 movable weight, 18 fixed microscope stage, 19 movable microscope stage, 20 micrometer screw, 21 pointer, 22 vernier, 23 head of microscope, 24 CCD camera, 25 computer, 26 frame grabber and 27 monitor.

Computerized unit: This is the fringe pattern analysis system, which consists of (23) head of microscope, (24) Panasonic CCD micro-camera, (25) PC, (26) digital frame grabber memory and (27) digital monitor.

This experimental set-up (Fig. 2) is used for determining the refractive index profile during the cold drawing of the PP fibres as follows. Firstly on the lower optical flat of the liquid wedge, a sample of certain length from PP fibres is fixed at one of its ends (at the interferometer) and the other end is linked with the clamp of the drawing system (see Fig. 2). A few drops of an immersion liquid (having refractive index close to that of the fibre) are put on this, fixed fibre. Then the fibre-drawing system is transferred to the optical interference system, where the wedge interferometer is fixed on the movable microscope stage. A parallel beam of polarized monochromatic light is used to illuminate at right-angles this liquid wedge interferometer, which is adjusted in such a way that the fibre axis is exactly perpendicular to the interference fringes in the liquid region.

The obtained fibre image (microinterferogram) is captured using the CCD camera and computerized unit. This image is digitized directly via the digitizer frame grabber that built in the computer. The digitized image is recorded on the computer storage media. This recorded microinterferogram is threshold enhanced and converted into a binary image to identify the contour line, which is analyzed via a software program [16] for the refractive index measurements of the fibre.

During the drawing process, the micrometer screw moves the drawing system, in particular the wedge interferometer, to a finite point (start point). This start point is 0.5 cm far from the fixed end of the fibre. The available part of the fibre length through the wedge is 2.5 cm; 25 microinterferograms along the fibre axis are captured and recorded using the computerized unit. That means the refractive index measurements of the PP fibre are obtained for each 1 mm from the available part of the fibre axis. Finally the previous step is repeated at different draw ratios and different positions along the fibre axis in case of light vibrating parallel and perpendicular to the fibre axis to obtain the fibre refractive indices $n^{\parallel}$ and $n^{\perp}$ measurements.

4. Results and discussion

The sample under investigation is undrawn PP fibres. The PP fibres are drawn in two different ways. The first one is termed *fast drawing*, in which the fibre is drawn with constant rate from initial state (undrawn) to the desired draw ratios (e.g. 1.3, 1.7 and 2). The second is termed *slow* (*step*) *drawing*, in which the fibre is drawn with increasing rate from initial state to the desired draw ratios (e.g. 1.1, 1.2, 1.3, 1.4,... and 2).

In the case of the fast drawing process, two samples of PP fibres are immersed in two suitable liquids of refractive indices ($n_L = 1.507$ and 1.499 close to $n^{\parallel}$ and $n^{\perp}$ of the fibre, respectively) at room temperature ($T = 26\,^{\circ}C$). Monochromatic light of wavelength $\lambda = 546.1$ nm was used. Some of the obtained microinterferograms for these fibres at different draw ratios ($D = 1$, 1.7 and 2) are illustrated in Fig. 3(a–f) in the case of light vibrating parallel and perpendicular to the fibre axis.

In the case of the slow drawing process, a sample of PP fibres is immersed in liquid of refractive index ($n_L = 1.502$) at room temperature ($T = 30\,^{\circ}C$) using the same wavelength. Fig. 4(a–g) shows the captured microinterferograms of the fibre at different draw ratios in case of light vibrating parallel and perpendicular to the fibre axis.

During each draw ratio, 25 microinterferograms are recorded at different positions along the fibre axis. It is found that in one of the deformation mechanisms that is called "smoothing mechanism" [22], there is a smooth change in the fibre optical properties with the draw ratio D and no change along the fibre axis. Except for draw ratios value ($D = 1.3$) in the case of the fast drawing, there is another type of deformation that is called "necking mechanism" as shown in Figs. 5 and 6 for light vibrating parallel and perpendicular to the fibre axis, respectively.

In qualitative details, when PP fibres are stretched or cold-drawn, they thin down at a point, resulting in the formation of "a neck". This necking occurs at the mechanical weak bonds and, due to the formation of voids or pores within the fibre structure, these neck zones are formed due to microscopic inhomogeneities

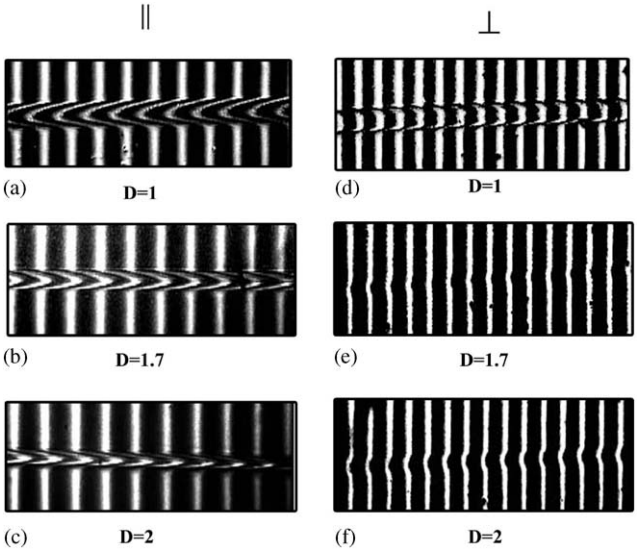

Fig. 3. Microinterferograms of PP fibres at different draw ratios (fast drawing) in the case of light vibrating parallel and perpendicular to the fibre axis using the automated system for producing multiple-beam Fizeau fringes in transmission at three different draw ratios (1, 1.7 and 2).

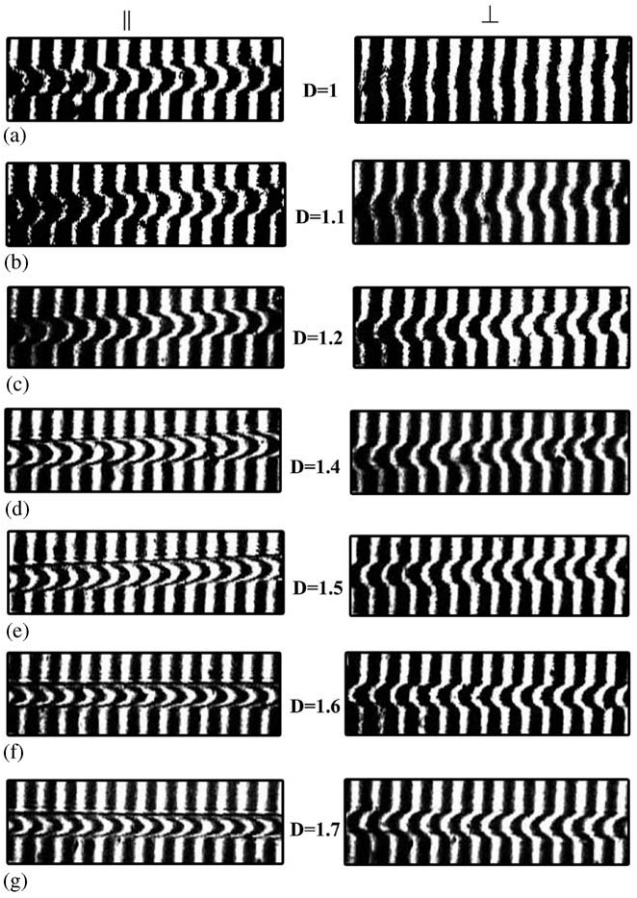

Fig. 4. Microinterferograms of PP fibres at different draw ratios (slow drawing) in the case of light vibrating parallel and perpendicular to the fibre axis using the automated system for producing multiple-beam Fizeau fringes in transmission.

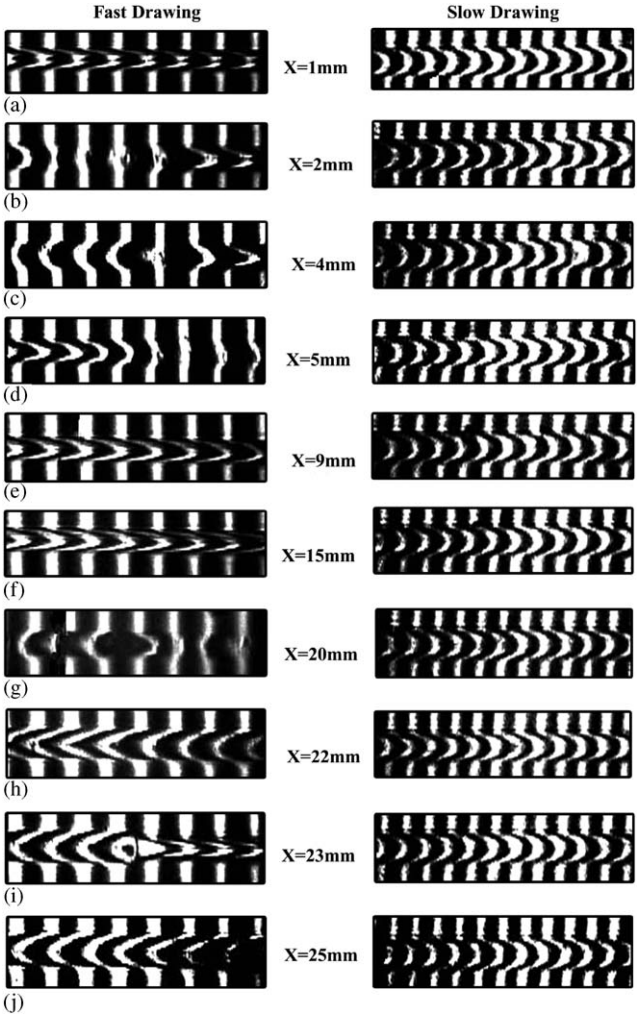

Fig. 5. Microinterferograms of PP fibres with draw ratio 1.3 (fast and slow drawing) at different positions along the fibre axis in the case of light vibrating parallel to this axis using the automated system for producing multiple-beam Fizeau fringes in transmission.

and, to a large extent, for the oriented polymer molecules [8,9]. Experimentally during the cold drawing, the necking deformation appears at different positions/regions along the fibre axis (see Figs. 5 and 6) when the heating rate of these regions exceeds the limit of flowing temperature of the molecular chains [23,24]. This excess of the fibre temperature results from the work done ($W' = F\Delta L$, where F is the drawing force and ΔL is the increment of fibre length) on the fibre chains during the cold-drawing process. Where the cold-drawing process associated with the release of quantity of heat that is equivalent to this work done, a part of this heat leads to heating the fibre and the other part is dissipated into the surrounding medium. The probability of the necking phenomenon increases by increasing each of the drawing rates and also increasing in the medium temperature. Accordingly, the predication of necking phenomena is mostly probable when (1) decreasing the temperature of drawing, (2) increasing the rate of drawing, and (3) increasing the fibre thickness.

Figs. 5 and 6 show a comparison between some of the obtained microinterferograms of PP fibres with draw ratio $D = 1.3$ in the case of the fast and slow drawing processes at different positions along the fibre axis. In the case of fast drawing, the various changes of fringe shift inside the fibre at different positions along the fibre axis occur due to the deformation of the fibre thickness, which established from the necking mechanism. In Fig. 5(a, e, f, and j) the left-hand-side LHS microinterferograms are recorded at positions $X = 1$, 9, 15 and 25 mm along the fibre axis, respectively, in which the fibre thickness is constant so that no changes in the fibre fringe shift. However, in the microinterferograms printed at the positions $X = 2$, 4, 5, 20, 22 and 23 mm, there are random and significant changes in the fibre fringe shift due to the obvious changes in the fibre thickness or necking deformation [see Fig. 5(i)]. In comparison (in case of slow/step drawing), it is clear that from the right-hand-side microinterferograms shown in Figs. 5 and 6 there is no significant change

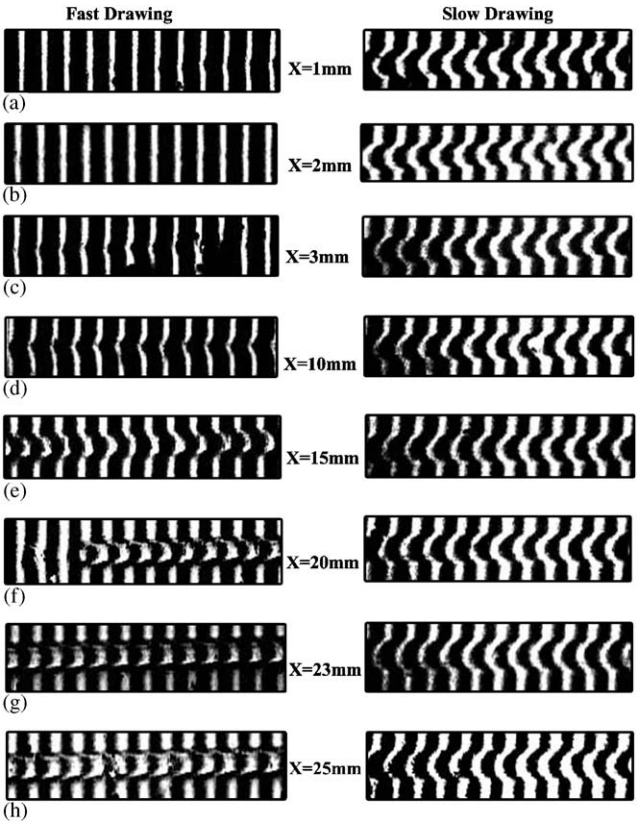

Fig. 6. Microinterferograms of PP fibres with draw ratio 1.3 (fast and slow drawing) at different positions along the fibre axis in the case of light vibrating perpendicular to this axis using the automated system for producing multiple-beam Fizeau fringes in transmission.

in the fringe shift inside the PP fibre due to constancy of the fibre thickness along the fibre axis.

In quantitative details, in the case of fast drawing, the mean refractive indices ($n^{\parallel}$ and $n^{\perp}$) of PP fibres are determined experimentally via the microinterferograms of Figs. 3–6 and the following Eq. [21]:

$$n^{j} = n_{\mathrm{L}} \pm \frac{Z^{j}\lambda}{2bt}, \tag{1}$$

where j denotes the state of light polarization $\parallel$ or $\perp$, n_{L} is the refractive index of the immersion liquid, Z is the maximum interference fringe shift inside the fibre, λ is the wavelength of the monochromatic light used, b is interfringe spacing, t is the fibre diameter and the sign ($\pm$) depends on the direction of the fringe shift Z inside the fibre.

In Fig. 7 the principal refractive index $n^{\parallel}$ of PP fibres is represented against the distance along the fibre axis at different draw ratios. It is found that there is no change in the values of $n^{\parallel}$ along the fibre axis and a smooth change with the draw ratios 1, 1.7 and 2. But the effect of necking deformation on the refractive index is clear at the draw ratio 1.3; also this effect is obvious in the case of $n^{\perp}$ as shown in Fig. 8. In the case of slow drawing, the refractive indices ($n^{\parallel}$ and $n^{\perp}$) are calculated using Eq. (1)

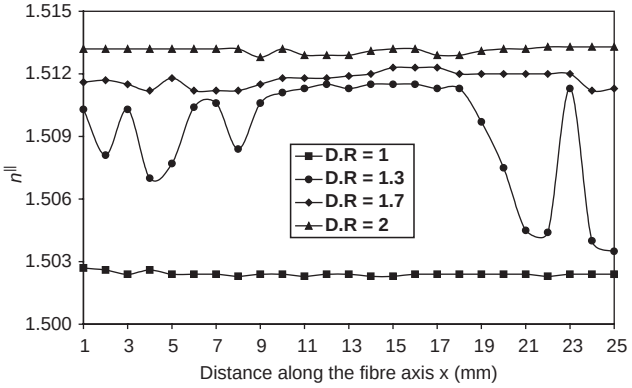

Fig. 7. Mean refractive index $n^{\parallel}$ of PP fibres against the distance along the fibre axis at different draw ratios (fast drawing).

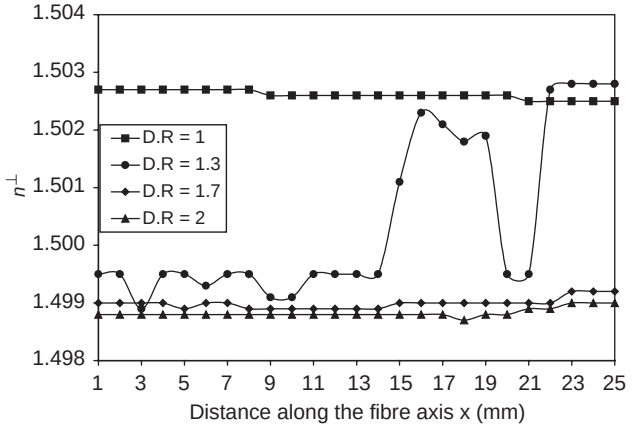

Fig. 8. Mean refractive index $n^{\perp}$ of PP fibres of PP fibres against the distance along the fibre axis at different draw ratios (fast drawing).

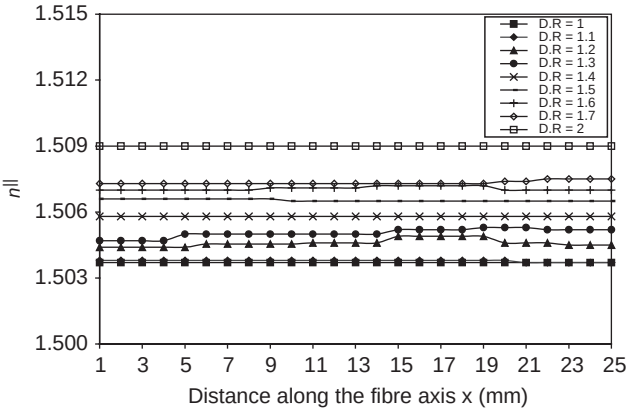

Fig. 9. Mean refractive index $n^{\parallel}$ of PP fibres against the distance along the fibre axis at different draw ratios (slow drawing).

and the microinterferograms of Figs. 4, 5 and 6, and results are given in Figs. 9 and 10, respectively. It is obvious that there are very small changes in the values of $n^{\parallel}$ and $n^{\perp}$ along the fibre axis and a smooth change with the draw ratios. Accordingly, it is clear that the

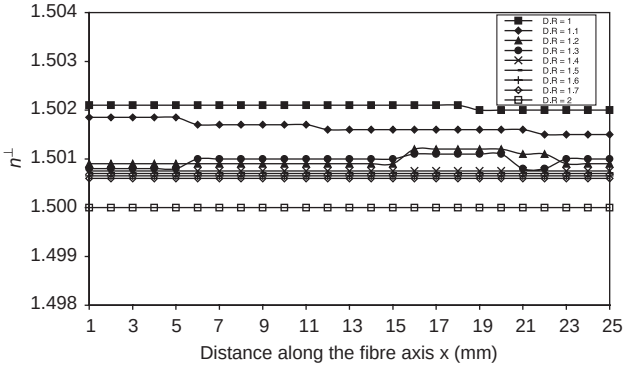

Fig. 10. Mean refractive index $n^{\perp}$ of PP fibres against the distance along the fibre axis at different draw ratios (slow drawing).

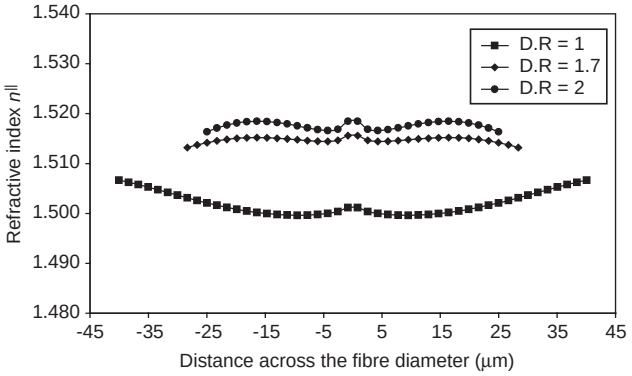

Fig. 11. Refractive index profile ($n^{\parallel}$) for PP fibres at different draw ratios (1, 1.7 and 2) in the case of the fast drawing process.

measured values of the mean refractive indices reflect the qualitative changes of the printed microinterferograms of the PP fibres. That is, ensure the effect of the necking and smoothing mechanisms during the comparative discussion between the fast and slow drawing processes.

To confirm the above results, specially in the case of fast drawing, the refractive index profiles for $n^{\parallel}$ and $n^{\perp}$ of PP fibres are determined at different draw ratios using the following Eq. [25,26]:

$$\frac{\lambda Z_Q}{2b} = \sum_{j=1}^{Q-1} 2n_j[K1 - K2] + 2n_Q K3 - n_0 K4, \qquad (2)$$

where $K1$, $K2$, $K3$ and $K4$ are given by

$$K1 = \sqrt{[R-(j-1)a]^2 - (d_Q n_0/n_j)^2},$$

$$K2 = \sqrt{(R-ja)^2 - (d_Q n_0/n_j)^2},$$

$$K3 = \sqrt{[R-(Q-1)a]^2 - (d_Q n_0/n_Q)^2},$$

$$K4 = \sqrt{R^2 - d_Q^2} + \sqrt{R^2 - X_Q^2},$$

where a is the layer thickness ($a = R/Q$), Q is the number of layers, d_Q is the distance between the incident beam and the fibre centre, X_Q is the distance between the emerging beam and the fibre centre and Z_Q is the fringe shift corresponding to the point X_Q in the multiple-beam interference pattern (microinterferogram).

Figs. 11 and 12 show these profiles that are computed using a software program based on Eq. (2) and the microinterferograms of Fig. 3 at the draw ratios 1, 1.7 and 2. At the draw ratio 1.3, the refractive index profiles ($n^{\parallel}$ and $n^{\perp}$) of PP fibres are plotted along the fibre axis as shown in Figs. 13 and 14, respectively. In Fig. 13 there is also significant variation in the refractive index profiles for $n^{\parallel}$ at different positions along the fibre axis. These variations may be classified into three groups of the refractive index profiles: the first (lower) group in which the fibre is considered undrawn and has refractive indices less than that of the immersion liquid (1.507), the

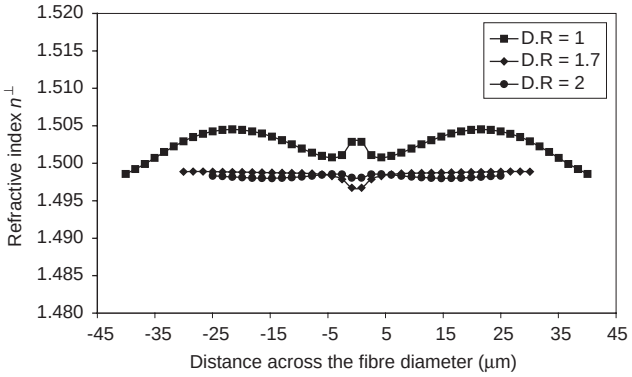

Fig. 12. Refractive index profile ($n^{\perp}$) for PP fibres at different draw ratios (1, 1.7 and 2) in the case of the fast drawing process.

second (middle) one in which the fibre is slightly drawn and has refractive indices that nearly match with that of the liquid and the third (upper) group in which the fibre is extremely drawn and has refractive indices more than that of the liquid. These variable profile groups are established due to the random changes of the fibre thickness, which is caused by the necking deformation along the fibre axis. Fig. 14 gives the same idea of Fig. 13 but for the perpendicular refractive index profiles ($n^{\perp}$).

From the above discussion, to avoid the occurrence of necking (deformation) mechanism during the cold drawing of PP fibres, the fibres must be cold drawn slowly in steps. In other words, the slow cold drawing for PP fibres is a preferred process instead of the fast cold drawing.

5. Conclusion

The automatic analysis of multiple-beam interference Fizeau fringes automatic analysis is used to obtain the refractive index profile of PP fibres. During the cold drawing, an accurate and fast software program is used for computing the fibre optical properties such as the principal refractive index and the refractive index profile

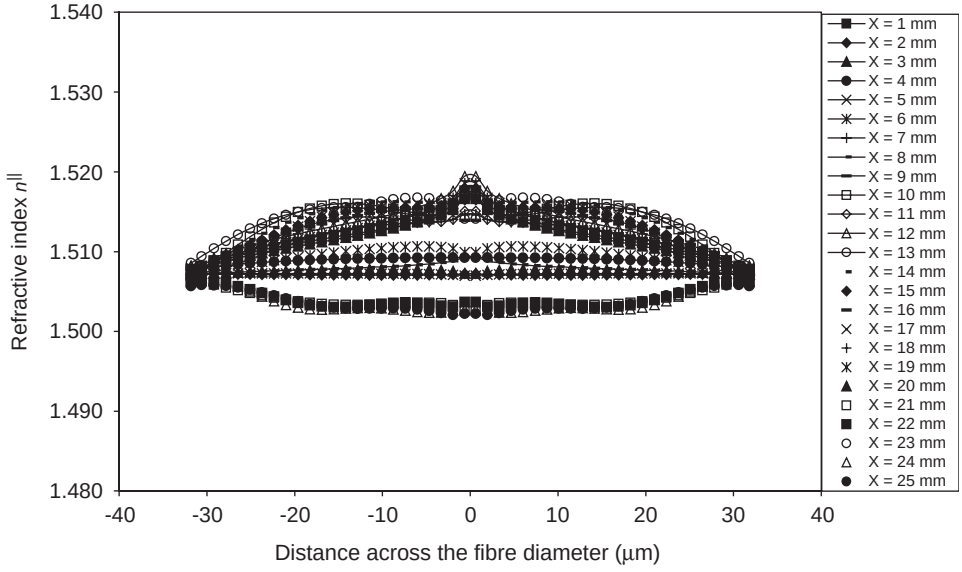

Fig. 13. Refractive index profile ($n^{\parallel}$) for PP fibres along the fibre axis at draw ratio 1.3 (fast drawing).

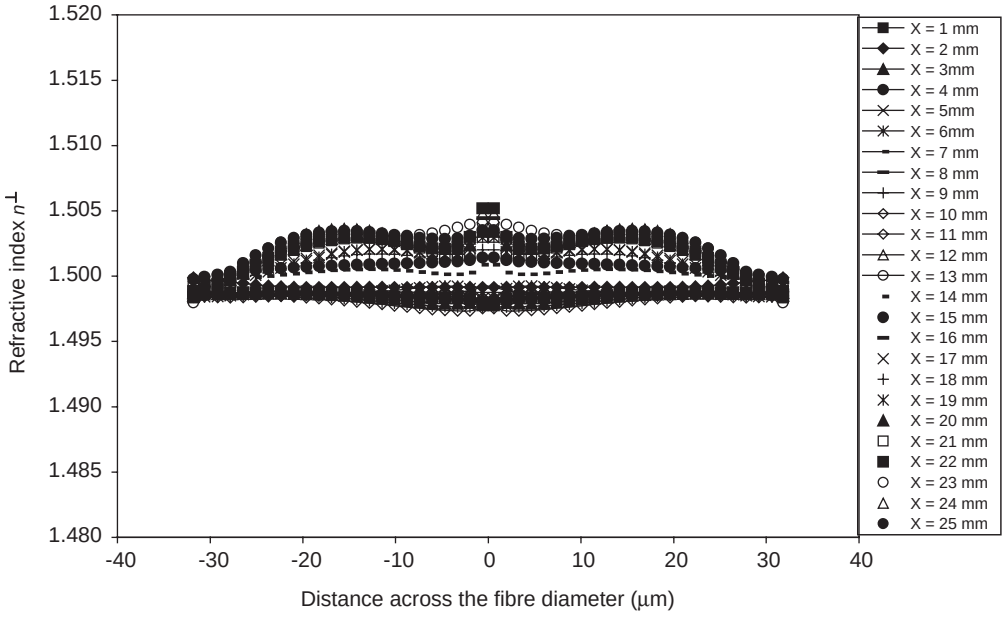

Fig. 14. Refractive index profile ($n^{\perp}$) for PP fibres along the fibre axis at draw ratio 1.3 (fast drawing).

at different positions along the fibre axis. The microinterferograms clearly identify differences in optical path variations due to the fibre drawing effect. The necking phenomenon can be predicted or avoided by controlling the degree of drawing (fast or slow) of the fibre. Hence the slow drawing process is recommended for use, which may be better than the fast one for drawing PP fibres to avoid the necking deformation. The described technique is efficient in evaluating and controlling the drawing process in synthetic fibres.

Acknowledgements

The authors wish to thank Prof. Dr. S. EL-Shalaby for helpful discussion throughout this work.

References

[1] Diakoumakos CD, Raptis I. Polymer 2003;44:251.
[2] de Candia F, Russo R, Tidjani A, Vittoria V, Peterlin A. J Polym Sci B: Polym Phys 1988;26:1897.
[3] Zhou H, Wilkes GL. J Mater Sci 1998;33:287.

[4] Hashimoto T, Kaisaki H, Kawal H. J Polym Sci: Polym Phys Ed 1978;16:271.
[5] Gilmore TF, Danis HA, Batra SK. Text Prog 1995;26(2): 24.
[6] Mabrouk MA. Polym Test 2002;21:897.
[7] Kontou E, Farasoglou P. J Mater Sci 1998;33:147.
[8] Walker J. Sci Am 1990:100.
[9] Sova M, Raab M, Sližová M. J Mater Sci 1993;28:6516.
[10] Carothers WH, Hill JW. J Am Chem Soc 1932;54:579.
[11] Peterlin A, Olf HG. J Polym Sci A-2 1966;4:587.
[12] Gent AN, Jeong J. Polym Eng Sci 1986;26:285.
[13] Gent AN, Madan S. J Polym Sci 1989;27:1529.
[14] Gent AN. Rubber Chem Technol 1996;69:59.
[15] Hamza AA, Fouda IM, El-Farahaty KA, Helaly SA. Polym Test 1987;7:329.
[16] Hamza AA, Sokkar TZN, Mabrouk MA, El-Morsy MA. J Appl Poly Sci 2000;77:3099.
[17] Leonov AI. J Rheol 1990;34:155.
[18] Kasei A, City N, Prefecture M, Lrish Scientist, Japan, 1999.
[19] Barakat N. Text Res J 1971;41:167.
[20] Hamza AA. Text Res J 1980;50:731.
[21] Barakat N, Hamza AA, Interferometry of Fibrous Materials, Hilger, Bristol, 1990.
[22] Mabrouk MA. Polym Test 2002;21:653.
[23] Jasbrich M, Diacik I, Faser U. Textile Techn 1967;18:331.
[24] Kobayashi J, Okajama S, Narita A. J Appl Polym Sci 1967;11(12):2515.
[25] Hamza AA, Sokkar TZN, Ghander AM, Mabrouk MA, Ramadan WA. Pure Appl Opt 1995;4:161.
[26] Hanns H, Kolloid ZZ. Polymer 1972;250:762.